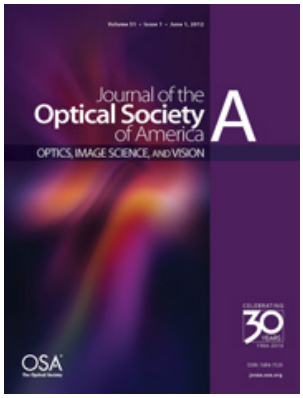

Rotation of the polarization direction and reversal of helicity of ultrashort pulsed beams propagating in free space

Balázs Major,[1,*] Miguel A. Porras,[2] and Zoltán L. Horváth[1]

[1] *Department of Optics and Quantum Electronics, University of Szeged, P. O. Box 406, Szeged H-6701, Hungary*

[2] *Departamento de Física Aplicada a los Recursos Naturales and Grupo de Sistemas Complejos, Universidad Politécnica de Madrid, Rios Rosas 21, Madrid ES-28003, Spain*

compiled: March 25, 2014

We unveil the origin of the recently revealed polarization state changes of polarization-shaped few-cycle pulses induced by free-space beam propagation. Simple rules are formulated to show how the orientation and ellipticity of the instantaneous polarization ellipse of the source and propagated pulses relate to each other. We demonstrate our findings with examples that clearly display the relationships found and highlight their relevance. We show, for example, that pulses often used in high-harmonic generation or attosecond pulse production rotate as a whole during free-space beam propagation or upon focusing. A pulse that may reverse its ellipticity from right-handed to left-handed during propagation is also introduced. It is shown that these effects are independent of the beam size and/or focal length. We also present how these instantaneous polarization state changes could be noticed in classical measurements of light polarization using polarizers, phase retarders and time-integrating detectors.

OCIS codes: *(320.2250) Femtosecond phenomena, (260.5430) Polarization, (030.1670) Coherent optical effects*

http://dx.doi.org/10.1364/XX.99.099999

1. Introduction

One of the most striking advances in optics in the last decades is the development of methods for the generation and shaping of pulses of light a few femtoseconds long, in which light frequencies spanning over the entire visible spectrum are coherently superposed. Sophisticated techniques allow to manipulate the individual frequencies, shaping the electric field at a femtosecond temporal scale [1, 2]. Moreover, polarization shaping techniques allow to generate femtosecond pulses whose polarization state (ellipticity and orientation of the instantaneous polarization ellipse) varies within the pulse in a precise way for their application in, for example, control of quantum systems, photochemistry, high-harmonic or attosecond pulse generation [3–5].

Suppose that such a polarization-shaped pulse is emitted by a planar source of finite area, and propagates in free space in the form of a highly directional beam. It is generally presumed that the polarization state is unaltered during propagation, particularly if the beam is wide. Similarly, it is not questioned in the experiments whether the instantaneous polarization state at a focus is equivalent to the state prior focusing [1–5].

* Corresponding author: bmajor@titan.physx.u-szeged.hu

It has been shown only recently that the polarization state of these polarization-shaped pulses may change on free-space propagation or focusing [6]. These changes can be approximately evaluated with the formulas given in Ref. [6]. However, the physical origin of this effect remains obscure. Indeed, the variations of the orientation and ellipticity of the instantaneous polarization ellipse in the examples in Ref. [6] seem accidental, and for this reason do not reveal the underlying reasons of this phenomenon. It would also be desirable to know whether these instantaneous polarization changes, which could only be measured by means of sophisticated techniques for the electric field reconstruction [7], has any reflect in polarization state changes measured classically using polarizers, phase retarders and time-integrating detectors [8].

In this paper we show that the change of the polarization state on free-space beam propagation follows a quite simple rule: a source pulse with a time-varying ellipticity at a given time results in a propagated pulse with a rotated instantaneous polarization ellipse at that time, and vice versa, a source pulse with a time-varying orientation of the polarization ellipse results in a propagated pulse with a shifted ellipticity. This effect is seen to originate in the contribution of Wolf's effect (change of the spectrum of light on propagation) that is due to the *finite extent* of the source, even in vacuum and if the

source is fully coherent [9, 10]. As such, these are more fundamental changes of the polarization state that must be distinguished from the ones that may additionally occur when the polarization is inhomogeneous across the source or when light is tightly focused [11], and from the changes of the partially polarized spectral components emitted by partially coherent sources [12–14]. Indeed, all spectral components of our polarization-shaped pulses are fully polarized, and their polarization state is unaltered during propagation.

We illustrate our results with two complementary examples, which clearly visualize the previously mentioned rules of instantaneous polarization-state changes. First, the "polarization gate" (PG) pulse [15], which is often used in attosecond pulse generation experiments [5], illustrates that propagation can induce a rotation of the pulse as a whole by many degrees because of its time-varying ellipticity, and that consequently, this effect is easily observable as a rotation of the direction of maximum fluence after a polarizer. Second, a "rotating" pulse [16], which shows that a pulse with a well-defined right-handed helicity (the same positive ellipticity at all instants of time) can result in a propagated pulse with a well-defined left-handed helicity, and that this change is directly observable in a classical measurement of the ellipticity.

2. Theoretical bases

2.A. Instantaneous polarization state

For the characterization of the instantaneous polarization state and its change on propagation, the complex electric field $\mathbf{E}(t) = E_x(t)\mathbf{u}_x + E_y(t)\mathbf{u}_y$ of a femtosecond pulse is seen to be conveniently expressed by means of its left-handed and right-handed circularly polarized orthogonal components as

$$\mathbf{E}(t) = E_l(t)\mathbf{u}_l + E_r(t)\mathbf{u}_r\,, \tag{1}$$

where $\mathbf{u}_l = (\mathbf{u}_x + i\mathbf{u}_y)/\sqrt{2}$ and $\mathbf{u}_r = (\mathbf{u}_x - i\mathbf{u}_y)/\sqrt{2}$. For a pulse of carrier angular frequency ω_0, we write $E_{x,y}(t) = \mathcal{A}_{x,y}(t)e^{-i\omega_0 t}$, or $E_{l,r}(t) = \mathcal{A}_{l,r}(t)e^{-i\omega_0 t}$, where the complex envelopes in the x-y and l-r representation relate by

$$\mathcal{A}_l(t) = \frac{1}{\sqrt{2}}[\mathcal{A}_x(t) - i\mathcal{A}_y(t)], \tag{2}$$

$$\mathcal{A}_r(t) = \frac{1}{\sqrt{2}}[\mathcal{A}_x(t) + i\mathcal{A}_y(t)]\,. \tag{3}$$

As is well-known, the complex envelopes, and therefore the real amplitudes $A_{l,r}(t) = |\mathcal{A}_{l,r}(t)|$ and phases $\Phi_{l,r}(t) = \arg[\mathcal{A}_{l,r}(\tau)]$, can be unambiguously determined from the electric field for pulses of duration (full width at half maximum of intensity) as short as a single optical period $T_0 = 2\pi/\omega_0$ [17]. The instantaneous polarization state of the pulse is then also unambiguously defined, and can be measured to the extent of experimental reconstructibility of the electric field [7]. In the l-r representation, the angle that the major axis of the instantaneous polarization ellipse forms with the laboratory x axis is given by

$$\psi(t) = \frac{[\Phi_r(t) - \Phi_l(t)]}{2}\,, \tag{4}$$

and the ellipticity $-\pi/4 \le \chi(t) \le \pi/4$ by

$$\tan\chi(t) = \frac{A_r(t) - A_l(t)}{A_r(t) + A_l(t)}\,, \tag{5}$$

positive (negative) ellipticity meaning right (left) helicity. For few-cycle pulses, the instantaneous polarization ellipse looses its interpretation as the temporal trajectory of the electric field, but retains its meaning as the geometrical locus of points occupied by the electric field when the pulse is subjected to phase transformations [6].

2.B. Pulsed beam propagation

Suppose a source at the plane $z = 0$ that emits the pulse $\mathbf{E}^{(s)}(t) = \mathbf{E}(t)U(r)$, where $U(r = \sqrt{x^2+y^2})$ limits the amplitude to a finite area. In a spectral approach to pulse propagation, the source spectrum $\hat{\mathbf{E}}^{(s)}(\omega) = \hat{\mathbf{E}}(\omega)U(r)$ is propagated using well-known laws of diffraction of monochromatic light. For a large source (whose linear dimensions are much larger than the wavelength $2\pi c/\omega$ for all relevant frequencies), diffraction is accurately described in a quasi-scalar, paraxial treatment, where the two transverse components $\hat{E}_{l,r}(\omega)U(r)$ are propagated independently, and the longitudinal component can be neglected. For the source spectrum $\hat{\mathbf{E}}^{(s)}(\omega) = \hat{\mathbf{E}}(\omega)U(r)$, the propagated spectrum adopts the form $\hat{\mathbf{E}}^{(p)}(\omega) = \hat{\mathbf{E}}(\omega)U(r,z,\omega)$, where $U(r,z,\omega)$ contains the spectral phase and amplitude acquired on propagation. For example, in the case of $U(r) = \exp(-r^2/s^2)$, standard Gaussian beam propagation formulas yield

$$U(r,z,\omega) = \frac{-iL(\omega)}{q(z,\omega)}\exp\left[\frac{i\omega r^2}{2cq(z,\omega)}\right]\exp\left[i\frac{\omega}{c}z\right]\,, \tag{6}$$

where $q(z,\omega) = z - iL(\omega)$ is the complex beam parameter and $L(\omega)$ is the Rayleigh range [18].

In time-domain, the complex electric field of the propagated pulse can then be retrieved from

$$\mathbf{E}^{(p)}(t) = \frac{1}{\pi}\int_0^\infty \hat{\mathbf{E}}(\omega)U(r,z,\omega)\exp\left(-i\omega t\right)\,, \tag{7}$$

and the propagated complex envelope of the left and right components from

$$\mathcal{A}^{(p)}_{l,r}(t) = \frac{1}{\pi}\int_0^\infty \hat{E}_{l,r}(\omega)U(r,z,\omega)\exp\left[-i(\omega-\omega_0)t\right]\,, \tag{8}$$

from which the polarization state can be extracted.

3. First-order approach to pulse propagation and instantaneous polarization change rules

To formulate simple rules for the propagation-induced changes of the instantaneous polarization state of femtosecond pulses, we apply the first-order approach developed in Ref. [18]. The effect of propagation on the

temporal shapes of the orthogonal components can be approximated by expanding the spectral phase acquired on propagation, $\varphi(r,z,\omega) = \arg[U(r,z,\omega)]$, and the spectral amplitude modification, $a(r,z,\omega) = |U(r,z,\omega)|$, about the central angular frequency ω_0 as $\varphi(\omega) \simeq \varphi_0 + \varphi_0'(\omega-\omega_0)$ and $a(\omega) \simeq a_0 + a_0'(\omega-\omega_0)$. In the preceding expressions (and throughout the article) prime signs denote differentiation with respect to ω, subscripts 0 evaluation at ω_0 (and the dependence of φ_0 and a_0 on r and z is omitted for conciseness). Proceeding as in Ref. [6], but for the l-r components instead of the x-y components, Eq. (8) leads to the approximate relation

$$\mathcal{A}_{l,r}^{(p)}(\tau) \simeq a_0 \mathcal{A}_{l,r}(\tau) \exp\left[i\frac{a_0'}{a_0}\frac{\mathrm{d}\ln \mathcal{A}_{l,r}(\tau)}{\mathrm{d}\tau}\right] \times \exp[i(\varphi_0 - \omega_0\varphi_0')] \quad (9)$$

between the source and propagated complex envelopes, where $\tau = t - \varphi_0'$ is the local time at the point (r,z). The source and propagated real amplitudes and phases are consequently related by

$$A_{l,r}^{(p)}(\tau) \simeq a_0 \exp\left[-\frac{a_0'}{a_0}\frac{\mathrm{d}\Phi_{l,r}(\tau)}{\mathrm{d}\tau}\right] A_{l,r}(\tau), \quad (10)$$

$$\Phi_{l,r}^{(p)}(\tau) \simeq \Phi_{l,r}(\tau) + \varphi_0 - \omega_0\varphi_0' + \frac{a_0'}{a_0}\frac{\mathrm{d}\ln A_{l,r}(\tau)}{\mathrm{d}\tau}, \quad (11)$$

which explicitly show a reshaping of the phases and amplitudes depending on each other for each component.

3.A. Rotation of the orientation

From Eqs. (11) and (4), the instantaneous orientation $\psi^{(p)}(\tau) = [\Phi_r^{(p)}(\tau) - \Phi_l^{(p)}(\tau)]/2$ of the polarization ellipse of the propagated pulse is

$$\psi^{(p)}(\tau) \simeq \psi(\tau) + \frac{1}{2}\frac{a_0'}{a_0}\frac{\mathrm{d}\ln[A_r(\tau)/A_l(\tau)]}{\mathrm{d}\tau}. \quad (12)$$

Using that, from Eq. (5), $\mathrm{d}\ln[A_r(\tau)/A_l(\tau)]/\mathrm{d}\tau = [2/(1-\tan^2\chi)][\mathrm{d}\tan\chi(\tau)/\mathrm{d}\tau]$, we obtain the result

$$\psi^{(p)}(\tau) \simeq \psi(\tau) + \frac{a_0'}{a_0}\frac{1}{1-\tan^2\chi(\tau)}\frac{\mathrm{d}\tan\chi(\tau)}{\mathrm{d}\tau}, \quad (13)$$

where the instantaneous orientation is seen to be rotated if the instantaneous ellipticity of the source pulse is time-varying.

In particular, far from and in front of quite general apertures $U(r)$, or at the focus of an ideal focusing system, the propagated spectrum has the form $\hat{E}_{l,r}^{(p)}(\omega) \propto -i\omega\hat{E}_{l,r}(\omega)\exp(i\omega z/c)$, meaning that the pulse is proportional to the time derivative of the source pulse [19]. The spectral amplitude is then filtered by $a(\omega) \propto \omega$, yielding $a_0'/a_0 = 1/\omega_0$ and a far field rotation

$$\psi^{(p)}(\tau) - \psi(\tau) \simeq \frac{1}{\omega_0}\frac{1}{1-\tan^2\chi(\tau)}\frac{\mathrm{d}\tan\chi(\tau)}{\mathrm{d}\tau} \quad (14)$$

that is independent of the source radius. The rotation vanishes when the characteristic time of variation of the ellipticity is much larger than the carrier period T_0, as for quasi-monochromatic light.

3.B. Change of the ellipticity

Reciprocally, the above approach predicts that a pulse with an instantaneous time-varying orientation of the polarization ellipse will change its instantaneous ellipticity on propagation. To evaluate the instantaneous ellipticity of the propagated pulse, we first note that, from Eq. (10),

$$A_r^{(p)}(\tau) \pm A_l^{(p)}(\tau) \simeq a_0 \exp\left[-\frac{a_0'}{a_0}\frac{\mathrm{d}\Phi_M(\tau)}{\mathrm{d}\tau}\right] \times \left\{[A_r(\tau) \pm A_l(\tau)] - \frac{a_0'}{a_0}\frac{\mathrm{d}\psi(\tau)}{\mathrm{d}\tau}[A_r(\tau) \mp A_l(\tau)]\right\}, \quad (15)$$

where we have written $\Phi_M(\tau) \equiv [\Phi_r(\tau) + \Phi_l(\tau)]/2$, and approximated $\exp[\pm(a_0'/a_0)(\mathrm{d}\psi/\mathrm{d}\tau)] \simeq 1 \pm (a_0'/a_0)(\mathrm{d}\psi/\mathrm{d}\tau)$. The ellipticity $\tan\chi^{(p)}(\tau) = [A_r^{(p)}(\tau) - A_l^{(p)}(\tau)]/[A_r^{(p)}(\tau) + A_l^{(p)}(\tau)]$ is then given by

$$\tan\chi^{(p)}(\tau) \simeq \frac{\tan\chi(\tau) - \dfrac{a_0'}{a_0}\dfrac{\mathrm{d}\psi(\tau)}{\mathrm{d}\tau}}{1 - \dfrac{a_0'}{a_0}\dfrac{\mathrm{d}\psi(\tau)}{\mathrm{d}\tau}\tan\chi(\tau)}, \quad (16)$$

or, keeping only terms up to the first order in a_0'/a_0, by

$$\tan\chi^{(p)}(\tau) \simeq \tan\chi(\tau) - \frac{a_0'}{a_0}[1-\tan^2\chi(\tau)]\frac{\mathrm{d}\psi(\tau)}{\mathrm{d}\tau}. \quad (17)$$

An instantaneous variation of the polarization ellipse orientation thus induces a variation in the instantaneous ellipticity upon propagation. In particular, at the far field or a focus, the ellipticity variation is

$$\tan\chi^{(p)}(\tau) - \tan\chi(\tau) \simeq \frac{1}{\omega_0}[1-\tan^2\chi(\tau)]\frac{\mathrm{d}\psi(\tau)}{\mathrm{d}\tau}, \quad (18)$$

which is independent of the source size and/or focal length, and vanishes for quasi-monochromatic pulses.

3.C. On the physical origin of the instantaneous polarization state changes

The above first-order approach indicates that the reason of the polarization state changes on propagation is a spectral amplitude filtering caused by diffraction. In more general terms, the change of the polarization state can be said to be due to the Wolf's effect, that is, the change of the spectral density on propagation [9]. Specifically, the change is by the reason of the finite size of the source [10].

The spectra $\hat{E}_{l,r}^{(s)}(\omega) = \hat{E}_{l,r}(\omega)U(r)$ of the two components at the source transform into $\hat{E}_{l,r}^{(p)}(\omega) = \hat{E}_{l,r}(\omega)U(r,z,\omega) \equiv \hat{E}_{l,r}(\omega)a(r,z,\omega)\exp[i\varphi(r,z,\omega)]$ on propagation, where $\varphi(r,z,\omega)$ is the spectral phase acquired on propagation, and $a^2(r,z,\omega)$ modifies the spectral densities $|\hat{E}_{l,r}(\omega)|^2$ of the two components. The dependence of $a(r,z,\omega)$ on ω reflects that the strength of diffraction depends on frequency, meaning that diffraction is a dispersive phenomenon. Filtering

both components with $a(r, z, \omega)$ does not alter the ratio $\hat{E}_l(\omega)/\hat{E}_r(\omega)$, and hence does not modify the polarization state of each spectral component (the ellipticity and orientation of the polarization ellipse of each spectral component), but alters differently the forms of $\hat{E}_l(\omega)$ and $\hat{E}_r(\omega)$ as functions of frequency (differently the size of the major axis of the spectral components), except when the two orthogonal components are strictly proportional (as in the case of a pulse with a time-independent polarization state), or unless the spectra of the two components are very narrow (as for a quasi-monochromatic pulse). In time domain, the two orthogonal components $E_l^{(p)}(t)$ and $E_r^{(p)}(t)$ are then changed differently, with the subsequent modification of the instantaneous polarization state.

4. Examples

These polarization changes were illustrated in Ref. [6] by means of a few example pulses. These were randomly chosen to have time-varying polarization orientation and time-varying ellipticity, which resulted in quite random changes in both the instantaneous orientation and instantaneous ellipticity on propagation, causing large pulse distortions and obscuring the underlying rules and their consequences written in Eqs. (13) and (17). In view of these rules, we first show that a pulse having an instantaneous polarization ellipse with time-independent orientation (so its polarization direction is well-defined and easily measurable) but possessing a time-varying ellipticity, rotates almost rigidly and gradually on propagation because of its finite transverse size. Second, we show that a pulse with a time-independent ellipticity but a time-varying ellipse orientation changes its ellipticity progressively on propagation, for example from positive to negative.

4.A. A pulse that rotates while propagating

Consider first the PG pulse

$$E_l(t) = A(t + \Delta t/2)\exp[-i\omega_0(t + \Delta t/2)]\,,$$
$$E_r(t) = A(t - \Delta t/2)\exp[-i\omega_0(t - \Delta t/2)]\,, \quad (19)$$

[Fig. 1(a)] whose left-handed and right-handed circularly polarized components are equal except that they are delayed by a small time Δt such that they partially overlap [15]. The ellipticity of the PG pulse changes gradually along the pulse from left-handed circular to linear at the middle of the pulse ($t = 0$), and then to right-handed circular. Choosing $A(t) = \exp(-t^2/\Delta T^2)$ for definiteness, the ellipticity grows monotonically from $-\pi/4$ to $+\pi/4$ as $\tan\chi(t) = \tanh[(\Delta t/\Delta T^2)t]$ [solid gray curve χ in Fig. 2(a)]. The instantaneous polarization ellipse maintains however the time-independent orientation $\psi = \Delta t\omega_0/2$ along the pulse [dashed black horizontal line ψ in Fig. 2(a)]. The PG pulse then has a well-defined polarization direction as a whole that can be easily observed: sending the PG pulse through a polarizer, a standard detector (such as a photodiode) placed behind it will provide the transmitted time-integrated

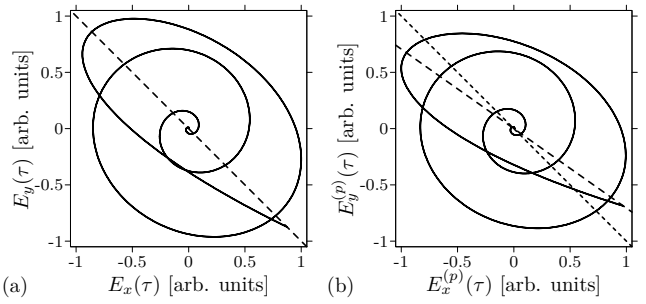

Fig. 1. Time evolution of the electric field of: (a) the PG pulse of carrier angular frequency $\omega_0 = 2.355$ fs^{-1} (800 nm carrier wavelength), Gaussian amplitude $A(t) = \exp(-t^2/\Delta T^2)$ of duration $\Delta T = 3.4$ fs (the intensity FWHM is 1.5 carrier cycles) and delay $\Delta t = 4.67$ fs (see Eq. (19)), (b) the PG pulse after propagation up to the far field, or to a focus, when the pulse is emitted by the source with $U(r) = \exp(-r^2/s^2)$. The straight dashed lines indicate the simulated direction of the polarizer resulting maximum transmitted fluence for the source and propagated PG pulse. For better comparison, a global phase $\pi/2$ has been added to the propagated pulse to eliminate the effect of Gouy phase shift $-\pi/2$ (it does not alter the state of polarization) on propagation from a finite source to the far field.

intensity, or fluence. As a function of the azimuthal angle θ of the polarizer, the transmitted fluence is given by $F(\theta) \propto 1 + \exp(-\Delta t^2/2\Delta T^2)\cos(2\theta - \Delta t\omega_0)$ [dashed curve θ in Fig. 2(b)], which has the appreciable contrast $\exp(-\Delta t^2/2\Delta T^2)$ (if the delay Δt is not large), and is maximum at the azimuthal angle $\theta_{\max} = \Delta t\omega_0/2$ equal to the orientation ψ of the ellipse.

Propagation of the PG pulse from the Gaussian aperture $U(r) = \exp(-r^2/s^2)$ up to the far field and in front of the aperture ($z \gg \omega_0 s^2/2c$, $r = 0$) is seen to result in the almost rigidly rotated PG pulse shown in Fig. 1(b). Similar rotation of equal magnitude [of about 10° counterclockwise in the example of Fig. 1] is observed for other choices of $U(r)$, for example, a hard circular aperture. The rotation of the pulse is a result of the rotation of the instantaneous polarization ellipse by approximately the same angle at all instants of time [solid black curve $\psi^{(p)}$ in Fig. 2(a)]. These values are close to the constant value $\psi^{(p)} - \psi \simeq \Delta t/\omega_0\Delta T^2$ predicted by Eq. (14) [dotted black line in Fig. 2(a)] from our first-order approach. At the same time, the instantaneous ellipticity is unaltered on propagation [dashed-dotted black curve $\chi^{(p)}$ in Fig. 2(a)], fitting also to the prediction $\tan\chi^{(p)}(\tau) = \tan\chi(\tau)$ of Eq. (18), since the instantaneous orientation is time-independent ($\mathrm{d}\psi/\mathrm{d}\tau = 0$). The expression $\psi^{(p)} - \psi \simeq \Delta t/\omega_0\Delta T^2$ also accounts for the facts that rotation vanishes for a linearly polarized pulse ($\Delta t = 0$), and is clockwise when the ellipticity decreases monotonically ($\Delta t < 0$).

The rotation of the instantaneous polarization ellipse at the far field is easily observable as shift of the azimuthal angle of maximum fluence transmitted through a polarizer placed at the far field by about the same

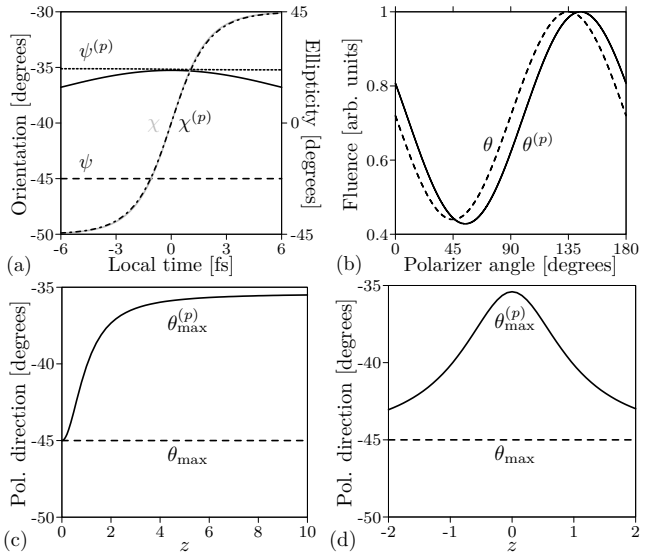

Fig. 2. (a) Time variation of the orientation (dashed black curve ψ) and ellipticity (solid gray curve χ) of the momentary polarization ellipse of the PG pulse in Fig. 1(a), and the same properties for the propagated PG pulse in Fig. 1(b) (solid black curve $\psi^{(p)}$ and dashed-dotted black curve $\chi^{(p)}$). The dotted black curve stands for the predicted polarization rotation by Eq. (13). (b) Simulated fluence after a polarizer for the PG pulse in Fig. 1(a) (dashed curve) and for the propagated pulse in Fig. 1(b) (solid curve) as a function of the transmission direction of the polarizer. (c) and (d) Simulated rotation of the direction $\theta_{\max}$ of polarizer yielding the maximum fluence behind it as a function of propagation distance z. For the collimated pulse in (c) the distance z is in units of the diffraction length $\omega_0 s^2/2c$, and for the focused pulse in (d) the distance z is measured from the focal point and is in units of the focal depth $2cf^2/\omega_0 s^2$.

angle as the rotation of the instantaneous ellipse [solid curve $\theta^{(p)}$ in Fig. 2(b)]. Figure 2(c) shows the gradual rotation of the direction $\theta_{\max}$ of polarizer yielding maximum fluence at increasing propagation distances from the source up to the far field. If as in most of the applications, the PG pulse is focused (the source amplitude $U(r)$ is multiplied by $\exp(-i\omega r^2/2cf)$), the same rotation effect is observed upon focusing. Figure 2(d) shows the gradual rotation on propagation, with a maximum rotation at the focal point equal to that at the far field, independently of the source radius and the focal length f.

Equation (13) also predict that these propagation-induced changes disappear when the typical scale of time-variation of the ellipticity is much larger than the carrier period. Figure 3(a) summarizes the values of the observable rotation $|\theta^{(p)}_{\max} - \theta_{\max}|$ of the PG pulse at the far field or at the focus when the pulse is scaled-up in time (increasing proportionally Δt and ΔT). In the limit of a quasi-monochromatic PG pulse, the rotation vanishes. At the typical durations of PG pulses used in experiments (for example, 10 fs), rotation is small but

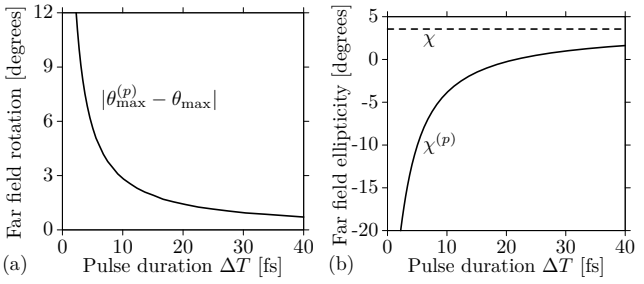

Fig. 3. (a) Rotation of the observable polarization direction of the PG pulse upon propagation up to the far field or a focus for different pulse durations. The time delay Δt is scaled proportionally with the pulse duration ΔT to retain a similar pulse shape ($\Delta t/\Delta T = \sqrt{2\ln 2}$), see Eq. (19). All other pulse properties are the same as in Fig. 1. (b) Ellipticity of the rotating pulse at the far field or at a focus for different pulse durations. During scaling pulse duration ΔT the product $\omega_d \Delta T$ is kept constant to retain similar pulse shape ($\omega_d \Delta T = \pi/\sqrt{2\ln 2}$), see Eq. (20). Note that this means that for small values of ΔT the $\omega_d \ll \omega_0$ assumption is not true. Other pulse properties are detailed later in Fig. 4.

still noticeable (about 3°).

We stress that the rotation of the instantaneous polarization direction at all times by approximately the same angle does not involve any rotation of the polarization direction of the spectral components. The spectra of the l and r components of the PG pulse in Eq. (19) are $\hat{E}_{l,r}(\omega) = \hat{A}(\omega)\exp(\mp i\omega\Delta t/2)$, where $\hat{A}(\omega)$ is the Fourier transform of $A(t)$. According to Eqs. (4) and (5) applied to a particular frequency, the spectral polarization ellipse orientation and ellipticity are $\psi(\omega) = \omega\Delta t/2$ and $\tan\chi(\omega) = 0$, that is, all frequencies are linearly polarized but along different directions. Similarly, the spectra of the l and r components of the propagated PG pulse are $\hat{E}^{(p)}_{l,r}(\omega) = \hat{A}(\omega)\exp(\mp i\Delta t\omega/2)a(r,z,\omega)\exp[i\varphi(r,z,\omega)]$, whose polarization orientation and ellipticity are also $\psi^{(p)}(\omega) = \omega\Delta t/2$ and $\tan\chi^{(p)}(\omega) = 0$, since the two orthogonal components are affected by the same factor $a(r,z,\omega)\exp[i\varphi(r,z,\omega)]$.

4.B. A pulse that reverses its helicity while propagating

Consider now the "rotating" pulse of components

$$E_l(t) = a_l A(t)\exp[-i(\omega_0+\omega_d)t]\,,$$
$$E_r(t) = a_r A(t)\exp(-i\omega_0 t)\,, \qquad (20)$$

[Fig. 4(a)]. It is a superposition of left- and right-handed circularly polarized pulses of slightly different frequencies ($\omega_d \ll \omega_0$) and amplitudes, characterized by the constant ellipticity $\tan\chi = (a_r - a_l)/(a_r + a_l)$ along the pulse, while the orientation of the ellipse $\psi(t) = \omega_d t/2$ is monotonously rotating, in a similar way as the pulse in Ref. [16]. With adequate choice of $a_l < a_r$, the ellipticity is slightly positive [dashed

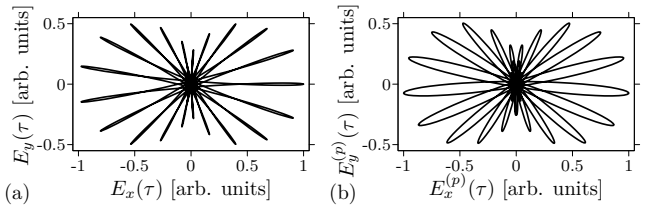

Fig. 4. Temporal evolution of the electric field of (a) the rotating pulse with $\omega_0 = 2.355$ fs^{-1} $\omega_d = 0.235$ fs^{-1}, Gaussian amplitude $A(t) = \exp(-t^2/\Delta T^2)$ of duration $\Delta T = 11.3$ fs, $a_l = 0.95$, and $a_r = 1.0$ (see Eq. (20)), and (b) of the rotating pulse after propagation up to the far field when the pulse is emitted by the source with $U(r) = \exp(-r^2/s^2)$.

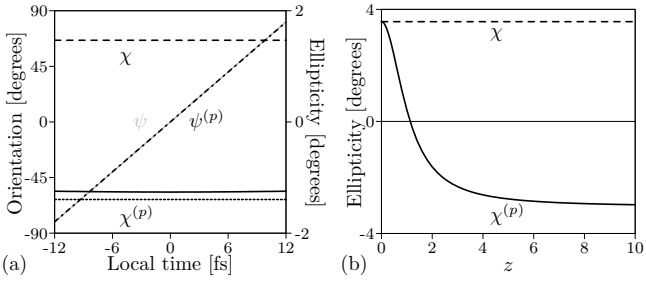

Fig. 5. (a) Temporal variation of the orientation (solid gray curve ψ) and the ellipticity (dashed black curve χ) of the instantaneous ellipse of the rotating pulse in Fig. 4(a), and the same properties for the propagated rotating pulse in Fig. 4(b) (dashed-dotted black curve $\psi^{(p)}$ and solid black curve $\chi^{(p)}$). The dotted black curve stands for the ellipticity prediction by Eq. (17). (b) Change of the ellipticity with propagation distance as it would be obtained by standard polarimetric techniques. The propagation distance z is in units of the diffraction length $\omega_0 s^2/2c$.

black curve χ in Fig. 5(a)]. At the far field, the approximate Eqs. (13) and (17) predict $\psi^{(p)}(\tau) \simeq \psi(\tau)$ and $\tan\chi^{(p)} \simeq (a_r - a_l e^{\omega_d/\omega_0})/(a_r + a_l e^{\omega_d/\omega_0})$. The ellipticity is still constant in time, but its value may be shifted to a negative value [dotted black curve in Fig. 5(a)]. Numerical evaluation of the propagated electric field with $A(t) = \exp(-t^2/\Delta T^2)$ [Fig. 4(b)] and of its instantaneous polarization state confirms that the ellipticity becomes negative at all times [solid black curve $\chi^{(p)}$ in Fig. 5(a)], and that the orientation is unchanged [solid gray curve ψ and dashed-dotted black curve $\psi^{(p)}$ in Fig. 5(a)].

Helicity reversal is clearly observable in a polarimetric measurement of the helicity. For example, the Stokes parameters can be determined by $s_0 = F(0,0) + F(90^\circ, 0)$, $s_1 = F(0,0) - F(90^\circ, 0)$, $s_2 = F(45^\circ, 0) - F(135^\circ, 0)$ and $s_3 = F(45^\circ, 90^\circ) - F(135^\circ, 90^\circ)$ [8], where

$$F(\theta,\epsilon) = \int_{-\infty}^{\infty} dt \{\mathrm{Re}[E^{(p)}(t,\theta,\epsilon)]\}^2 = \frac{1}{2}\int_{-\infty}^{\infty} dt |E^{(p)}(t,\theta,\epsilon)|^2 \tag{21}$$

is the measured time-integrated intensity of the transmitted electric field $E^{(p)}(t,\theta,\epsilon) = E_x^{(p)}(t)\cos\theta + E_y^{(p)}(t)e^{i\epsilon}\sin\theta$ after a polarizer of azimuthal angle θ, and a retarder causing ϵ phase shift [8]. Evaluation of the ellipticity $\sin(2\chi^{(p)}) = s_3/\sqrt{s_1^2 + s_2^2 + s_3^2}$ from the numerically propagated field at increasing distances z [solid curve in Fig. 5(b)] shows its change from right- to left-handed values [from $\chi = +3.6^\circ$ at the source to $\chi^{(p)} = -3.0^\circ$ at far field in Fig. 5(b)].

As in the case of the PG pulse, these observable polarization changes vanish in the limit of long pulses. In Fig. 3(b) the ellipticity at the far field or a focus is seen to approach its original value at the source when the rotating pulse is scaled-up in time so that it becomes quasi-monochromatic.

5. Summary and concluding remarks

To summarize, our study has shown that the polarization state of polarization-shaped ultrashort pulses can change during free-space beam propagation due to the different reshaping of the spectra of the orthogonal components when the source has a finite extent. Along with revealing the source of these changes, we have found simple rules to predict the propagation-induced variations of the instantaneous polarization state, provided that they are small. These rules show that the correlation between the parameters of the instantaneous polarization ellipse is the following: time-varying ellipticity causes orientation rotation during propagation, and vice versa, if the orientation changes in time, the ellipticity is shifted on propagation.

We used two examples to demonstrate our findings. The first example is a pulse generally used for isolated attosecond pulse generation. The above rules imply that this pulse rotates as a whole upon propagation up to the far field or to a focus. Based on the fact that the high harmonic generation efficiency depends on the polarization state of the fundamental field, this phenomenon could have an effect on the outcome of these experiments. A variant of the second example has been proposed to measure the carrier-envelope phase. In this case, the ellipticity shifts from positive to negative on propagation. All these changes are predicted to be easily observable in standard measurements of the polarization state. We have also found that at the far field or at the focus of an ideal focusing system these effects are independent of the source shape, size and/or the focal length, being solely determined by the polarization-shaped structure of the pulse.

We suspect, to conclude, that these easily observable polarization changes have gone unnoticed because they are not expected. Also, since the development of a unified theory of partial coherence and polarization, polarization changes are expected in connection with partially coherent sources, and studies focus on the spectral polarization changes of stationary random beams [12–14]. For a deterministic pulse, the spectral polarization state is indeed invariant, being the instantaneous polarization state that becomes relevant experimentally.

6. Acknowledgments

The work of B. M. was supported by the European Union and the State of Hungary, co-financed by the European Social Fund in the framework of TÁMOP-4.2.4.A/2-11/1-2012-0001 'National Excellence Program'. M. A. P. acknowledges financial support from Project MTM2012-39101-C02-01 of Ministerio de Economía y Competitividad of Spain.

References

[1] S. Cundiff and A. Weiner, "Optical arbitrary waveform generation," Nat. Photonics **4**, 760–766 (2010).

[2] M. Th. Hassan, A. Wirth, I. Grguraš, A. Moulet, T. T. Luu, J. Gagnon, V. Pervak, and E. Goulielmakis, "Invited Article: Attosecond photonics: Synthesis and control of light transients," Rev. Sci. Instrum. **83**, 111301 (2012).

[3] T. Brixner, G. Krampert, T. Pfeifer, R. Selle, G. Gerber, M. Wollenhaupt, O. Graefe, C. Horn, D. Liese, and T. Baumert, "Quantum Control by Ultrafast Polarization Shaping," Phys. Rev. Lett. **92**, 208301 (2004).

[4] L. Polachek, D. Oron, and Y. Silberberg, "Full control of the spectral polarization of ultrashort pulses," Opt. Lett. **31**, 631–633 (2006).

[5] I. J. Sola, E. Mével, L. Elouga, E. Constant, V. Strelkov, L. Poletto, P. Villoresi, E. Benedetti, J.-P. Caumes, S. Stagira, C. Vozzi, G. Sansone, and M. Nisoli, "Controlling attosecond electron dynamics by phase-stabilized polarization gating," Nat. Phys. **2**, 319–322 (2006).

[6] M. A. Porras, "Propagation-induced changes in the instantaneous polarization state, phase, and carrier–envelope phase of few-cycle pulsed beams," J. Opt. Soc. Am. B **30,** 1652–1659 (2013).

[7] L. Xu, P. Schlup, O. Masihzadeh, R. A. Bartels, and R. Trebino, "Analysis of the measurement of polarization-shaped ultrashort laser pulses by tomographic ultrafast retrieval of transverse light E fields," J. Opt. Soc. Am. B **26**, 2363–2369 (2009).

[8] M. Born and E. Wolf, *Principles of Optics*, 7th ed. (Cambridge University Press, 1999).

[9] E. Wolf, "Invariance of the Spectrum of Light on Propagation," Phys. Rev. Lett. **56,** 1370–1372 (1986).

[10] Z. Dačić and E. Wolf, "Changes in the spectrum of a partially coherent light beam propagating in free space," J. Opt. Soc. Am. A **5,** 1118–1126 (1988).

[11] L. E. Helseth, "Strongly focused polarized light pulse," Phys. Rev. E **72,** 047602 (2005).

[12] D. F. V. James, "Change of polarization of light beams on propagation in free space," J. Opt. Soc. Am. A **11**, 1641–1643 (1994).

[13] E. Wolf, "Unified theory of coherence and polarization of random electromagnetic beams," Phys. Lett. A **312**, 263–267 (2003).

[14] O. Korotkova and E. Wolf, "Changes in the state of polarization of a random electromagnetic beam on propagation," Opt. Commun. **246,** 35–43 (2005).

[15] D. Oron, Y. Silberberg, N. Dudovich, and D. M. Villeneuve, "Efficient polarization gating of high-order harmonic generation by polarization-shaped ultrashort pulses," Phys. Rev. A **72,** 063816 (2005).

[16] M. Kakehata, Y. Kobayashi, H. Takada, and K. Torizuka, "Single-shot measurement of a carrier-envelope phase by use of a time-dependent polarization pulse," Opt. Lett. **27,** 1247–1249 (2002).

[17] T. Brabec and F. Krausz, "Nonlinear Optical Pulse Propagation in the Single-Cycle Regime," Phys. Rev. Lett. **78,** 3282–3285 (1997).

[18] M. A. Porras, "Diffraction effects in few-cycle optical pulses," Phys. Rev. E **65,** 026606 (2002).

[19] G. C. Sherman, "Short pulses in the focal region," J. Opt. Soc. Am. A **6,** 1382–1387 (1989).